

## Mechanical Behavior of Bulk Amorphous Alloys Reinforced by Ductile Particles at Cryogenic Temperatures

Cang Fan,<sup>1</sup> Hongqi Li,<sup>1</sup> Laszlo J. Kecskes,<sup>2</sup> Kaixiang Tao,<sup>1</sup> Hahn. Choo,<sup>1</sup> P. K. Liaw,<sup>1</sup> and C. T. Liu<sup>1</sup>

<sup>1</sup>Department of Materials Science and Engineering, University of Tennessee, Knoxville, Tennessee 37923, USA

<sup>2</sup>U.S. Army Research Laboratory, Aberdeen Proving Ground, Maryland 21005, USA

(Received 24 January 2006; published 14 April 2006)

The mechanical behavior of Zr-based bulk amorphous alloy composites (BAACs) was investigated at 77 K. The 5 vol. % Ta-BAAC maintained large plastic strains of  $\sim 13\%$  with a 16% strength increase, when compared with that at 298 K. The interaction between shear bands and particles shows that shear extension in particles has limited penetration, and shear bands build up around particles. In addition to on the failure surface of the amorphous matrix, molten characteristics were also found on the surface of sheared particles. Pair distribution function studies were performed to understand the mechanical behavior.

DOI: 10.1103/PhysRevLett.96.145506

PACS numbers: 62.20.Fe, 61.12.-q

Polycrystalline solids with bcc or hcp structure normally exhibit a ductile to brittle transition (DBT) as the temperature decreases. This is a result of high lattice friction stresses (Peierls stresses) in bcc and hcp. By contrast, fcc metals generally remain ductile at low temperatures. However, it remains unknown whether amorphous alloys, which have no dislocation, also exhibit a DBT at cryogenic temperatures, such as at the liquid nitrogen temperature (77 K).

Amorphous alloys have microstructures which do not exhibit long range order and exhibit several unique properties, such as high strength (up to 4 GPa) and large elastic elongation ( $\sim 2\%$ ), as well as low plasticity (less than 1%) to failure [1,2]. The *in situ* nanosized to microsized crystalline reinforced bulk amorphous alloy (BAA) composites (BAACs) exhibit both improved strength and plasticity (more than 12%) [3–11], which significantly increases their commercial viability. Except at cryogenic temperatures, amorphous alloys and their composites at room and high temperatures have been widely studied [1,2,12,13].

Shear bands are important in BAAs and BAACs, because the associated work softening leads to plastic instability, limiting the potential of BAAs and BAACs as structural materials. Direct temperature measurements are hindered by the localization and extremely short duration of the shear ( $10^{-5}$  s). Infrared imaging has been used to estimate rises of 650–1200 K within the bands [14]. More recently, Lewandowski and Greer presented that the temperature rise can be as high as a few thousand Kelvin by the studies of a fusible tin coating [15]. It is of interesting to investigate such a high temperature rise experimentally.

Master alloys were prepared by arc melting through a normal procedure [16] for  $Zr_{60}Cu_{30}Al_{10}$  (in atomic percent) and a two-step procedure [3,16] for *in situ* Ta-particle-reinforced  $(Zr_{55}Ni_{10}Cu_{20}Ta_3Al_{12})_{96}Ta_4$  BAAC (Ta-containing BAAC hereafter). Cylindrical rods, which include a specially designed composite that contains Ta wire

of 0.5 mm in diameter existing in the center of a BAA to investigate the sheared Ta, were cast into a copper mold with dimensions of 3 mm in diameter and 75 mm in length. 70 vol. % (volume fraction) W-particle-containing-Vit106 BAAC [17] (W-containing BAAC hereafter) were received from the U.S. Army Research Laboratory. Uniaxial compression tests were conducted on specimens with 6 mm lengths and 3 mm diameters, in different temperatures at a strain rate of  $1 \times 10^{-3} s^{-1}$ .

Mechanical properties of W-containing-BAAC samples were measured at 693, 298, and 77 K. As shown in Fig. 1(a), the plastic strains decrease significantly upon lowering the testing temperature, i.e., over 110% (stopped test) at 693 K, about 58% at 298 K, and 20% at 77 K, while the yield strengths increase significantly, i.e., 390 MPa at 693 K, 930 MPa at 298 K, and 1300 MPa at 77 K, respec-

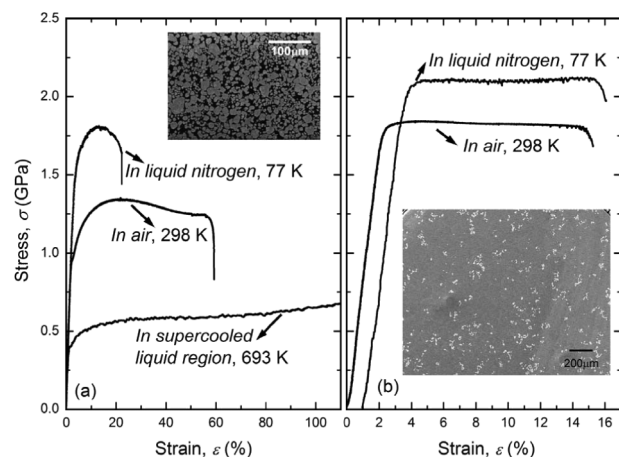


FIG. 1. The true stress-strain curves measured at 77 and 298 K (a) as well as in the supercooled liquid region, 693 K for 70 vol. % W-containing-Vit106 BAACs with the SEM image and (b) for 5 vol. % Ta-containing Zr-based BAACs with the backscattering SEM image.

tively. Strain hardening, which was from W particles, appears at the three temperatures. However, a reduction in stresses is noted after 26% strain for the sample tested at 298 K and 16% for 77 K. By contrast, as shown in Fig. 1(b), the investigation on Ta-containing BAAC shows increased strength with unchanged plastic strain of  $\sim 13\%$  upon lowering the testing temperature from 298 to 77 K. The yield and maximum strengths obtained at 298 K are about 1760 and 1830 MPa, whereas at 77 K they are about 2040 and 2120 MPa—a 16% increase. The Ta-containing BAAC exhibits excellent mechanical properties at the cryogenic temperature. Therefore, we focus on this material to investigate their failure characteristics, especially the interaction between shear bands and particles.

The failure surface, shear bands, and their interaction with particles in the Ta-containing-BAAC samples were investigated by scanning electron microscopy (SEM) as shown in Fig. 2. Large numbers of shear bands appear on both samples, of which they were measured at 298 and 77 K [Figs. 2(a) and 2(b)]. They are much denser than monolithic bulk amorphous alloys [10]. If we investigate the failure surfaces as shown in Fig. 2(c), we can see that two kinds of vein patterns can be found. One is marked as area *A*, which is rougher with lots of molten liquidlike droplets, and the other one is area *B*, which is smoother. If we look at the Ta particles, they are all sheared in one direction (downwards), and the vein patterns appear on the top of the sheared Ta and are continuous with that of the amorphous matrix. These vein patterns can be formed either by spreading over from the molten amorphous ma-

trix or the Ta particles themselves—they have even been melted.

The interaction between particles and shear bands was also investigated. As shown in Fig. 2(d), the backscattered SEM image of a number of shear bands reveals limited extension and multiple branching during deformation, even in the area of  $20 \times 20$  microns squared. The shear bands *B* and *C* are around and extended into the Ta-1 particle in the form of shear zones but do not propagate through the Ta-1 particle or emerge on the other side of the particle and do not reach the Ta-2 particle. The shear band traversed into a Ta-1 particle deformed as sheared zone *E* with limited length; as a result, it shears off the Ta-1 particle as pointed out by arrow *F*. These deformation characteristics are significantly different from that of the monolithic BAAs, in which shear bands traverse the entire sample [1,2,10,11]. The limited length of the shear bands and sheared zone inside and around the Ta-1 particle indicates that shear bands are both initiated and absorbed at the ductile precipitate and, thus, contribute to enhanced plasticity. The shear-band-like contrast inside the precipitate seems to be related to dislocations.

To further investigate the source of the vein patterns appearing on the top of the sheared Ta particles, we used the BAA samples that contain Ta wire. The sample failed after limited plastic strain ( $<0.1\%$ ). As shown in Fig. 3(a), three areas of *A*, *B*, and *C* can be found on the Ta failure surface. Figure 3(b) shows the enlarged area *A*, in which it shows the molten vein patterns and liquidlike droplets. The shear direction is upwards, and the area *A* is formed by almost purely shearing deformation. The enlarged area *B* is shown in Fig. 3(c), in which it shows molten droplets and a

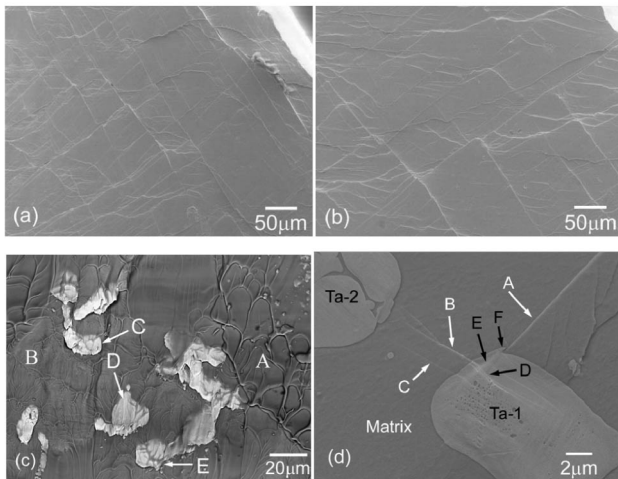


FIG. 2. The SEM images of shear bands appear on the side surface of the compressed sample (a) at 298 K and (b) at 77 K; the backscattering SEM images at 77 K showing (c) vein patterns of a more melted area *A* and less melted area *B* on a failed amorphous surface, as well as on the surface of sheared Ta particles *C*, *D*, and *E*; and (d) the interaction between shear bands and particles. The investigated samples were 5 vol. % Ta-containing Zr-based BAACs.

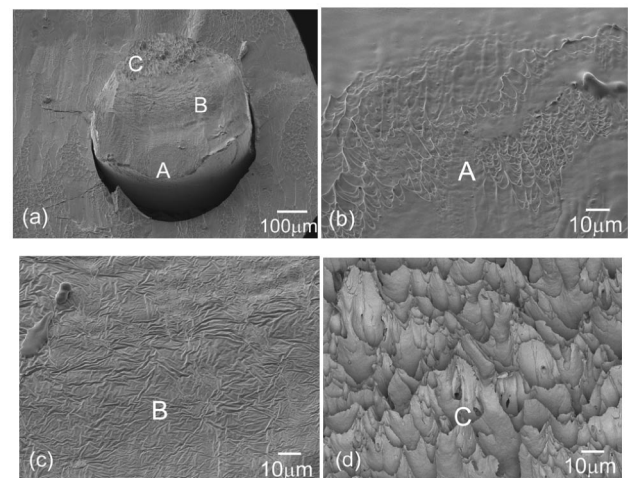


FIG. 3. SEM images of sheared failure surfaces for as-cast  $Zr_{60}Cu_{30}Al_{10}$  BAA containing Ta wire with the dimension of 0.5 mm in diameter. (a) Different failure characteristics of *A*, *B*, and *C* on a failure Ta surface; (b) molten vein pattern of enlarged area *A*; (c) molten smoother pattern of enlarged area *B*; and (d) ductile failure surface of enlarged area *C*.

molten surface that is much smoother than that in area A. Because of the sheared plastic deformation that propagates from one side of A to the other side of C in the Ta wire by dislocation deformation mold, area B should be deformed under mixing loading conditions, such as mixed shearing and tensile conditions. When the deformation propagates to area C, in which a tensile condition might be a dominating factor, it fails under the character of typical failure future on Ta under tension. The results of the molten character on Ta wire indicate that the temperature can rise up over the Ta melting temperature ( $T_m = 3293$  K) in the shear bands.

In order to estimate the cryogenic effect at the atomic level, pair distribution function (PDF) analyses of as-cast ternary  $Zr_{60}Cu_{30}Al_{10}$  BAAs, which have a comparable limited plastic strain and  $\sim 16\%$  increase in strength from 298 to 77 K, were performed at 15 and 298 K using the Neutron Powder Diffractometer (NPDF) at the Los Alamos National Laboratory. The powder diffraction data were collected over a wide range (up to  $51.1 \text{ \AA}^{-1}$ ) of  $Q$  ( $Q = 4\pi \sin\theta/\lambda$ ). The PDF  $G(r)$  was computed by PDFGETN [18] from the Fourier transform of  $Q[S(Q) - 1]$  [19]:

$$G(r_k) = 2/\pi \sum Q_j [S(Q_j) - 1] \sin(Q_j r_k) \Delta Q_j. \quad (1)$$

Figure 4 shows the results of their PDFs  $G(r)$  vs  $r$ , where  $r$  is the distance between pairs. The intensities of the peak around 2.78 and 3.05  $\text{\AA}$  of the PDF from 298 to 15 K increased slightly and narrowed slightly, and the FWHM (full width at half maximum) of the peaks decreased only 5%–7%. This result indicates that thermal vibrations in the amorphous state are much smaller than in the crystalline phase [19]; for example, in results from  $CuZr_2$ , the crystallized stable phase shows 30%–45% reduction in the FWHM [20]. It is also the reason the strength increased a

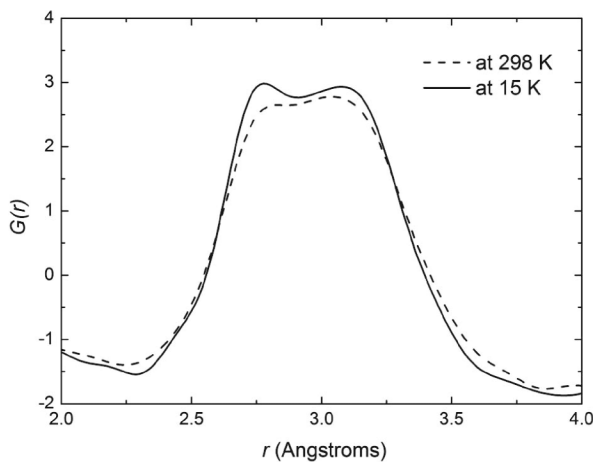


FIG. 4. Pair distribution function measured at room temperature (dashed line) and 15 K (solid line) for as-cast  $Zr_{60}Cu_{30}Al_{10}$  bulk metallic glass.

few percent (16%) for the 5 vol. % Ta-containing BAAC than that (40%) for the 70 vol. % W-containing-Vit106, since the increases of the strength upon lowering the temperature are caused mainly by reduced thermal vibrations.

Then what is the reason for the different changes in plastic behaviors of the two composites shown in Fig. 1? As shown in Fig. 3, at the amorphous matrix and Ta particle interface, a stress concentration exists. Because of its lower yield strength, the ductile particle yields prior to the yielding of the matrix, with the introduction of internal dislocations. As such, upon compression, this increasing stress mismatch between the matrix and the particles could be considered to be the reason for the particle-matrix interface being an initiation site for shear band formation. Obviously, the initiation and absorption of shear bands by particles would result in an increasing number of shear bands arising during deformation [3]. Consequently, the ductility of the particles is the dominating factor on shear band deformation. Even when the particles are brittle, they can still initiate shear band but lose the ability to absorb them. In this case, unlike that shown in Fig. 3(d), the shear bands can go through brittle particles easily and cause samples to fail prematurely. W has bcc structure and has a DBT temperature (DBTT) in the range of 253–323 K [21]. Therefore, the W particles in W-containing-Vit106 result in significantly reduced plasticity at cryogenic temperature. The Ta particles also have bcc structure, but Ta does not show DBTT even when the temperature is lowered to 30 K [21]. Therefore, the Ta particles can perform similarly at 298 and 77 K on shear band initiation and propagation.

From the results above, essentially, the amorphous matrix does not exhibit DBTT when lowered to 77 K. We attempt to determine the relationship between the amorphous structures and their shear band propagation through a model that we have recently constructed [20]. In this model, strongly bonded clusters, acting as units, are randomly distributed and strongly connected to each other. The combined bonding types and properties of such clusters, and the connections between the clusters, provide strength and ductility. The spaces between clusters form free volume, which possibly provides room for the motion or rotation of clusters. The cooperatively rotating clusters form a layer motion, which is  $\sim 20$  nm [22,23], and this deforms the amorphous alloys upon applied loading. Because of the fact that the FWHM of the nearest atomic pairs in PDFs, from 298 to 15 K, decreased only 5%–7%, the shear band motion has essentially no change. Therefore, similar shear band deformation occurs in this temperature region.

The above results indicate that the BAAs and BAACs have integrated excellent mechanical properties in liquid nitrogen. They can be potentially promising for cryogenic temperature or space applications.

C.F. acknowledges valuable discussions with T.W. Wilson, T.G. Nieh, and T. Hufnagel and thanks G.Y. Wang for assistance with the high temperature mechanical testing. This work was supported by the National Science Foundation, the International Materials Institutes (IMI) Program under Grant No. DMR-0231320. This work has benefited from the use of NPDF at the Lujan Center at Los Alamos Neutron Science Center, Los Alamos National Laboratory, funded by the Department of Energy under Contract No. W-7405-ENG-36 (the upgrade of NPDF has been funded by NSF through Grant No. DMR 00-76488). C. T. L. is supported by the Division of Materials Science and Engineering, Office of Basic Energy Sciences, U.S. Department of Energy, under Contract No. DE-AC05-00OR-22725 with UT-Battelle, LLC.

- 
- [1] W. L. Johnson, MRS Bull. **24**, 42 (1999).  
[2] A. Inoue, *Uetikon-Zuerich* (Trans Tech Publications, Switzerland, 1998).  
[3] C. Fan, R. T. Ott, and T. C. Hufnagel, Appl. Phys. Lett. **81**, 1020 (2002).  
[4] C. C. Hays, C. P. Kim, and W. L. Johnson, Phys. Rev. Lett. **84**, 2901 (2000).  
[5] C. Fan, A. Takeuchi, and A. Inoue, Mater. Trans., JIM **40**, 42 (1999).  
[6] C. Fan and A. Inoue, Mater. Trans., JIM **38**, 1040 (1997).  
[7] M. Calin, J. Eckert, and L. Schultz, Scr. Mater. **48**, 653 (2003).  
[8] C. Fan, D. V. Louzguine, C. F. Li, and A. Inoue, Appl. Phys. Lett. **75**, 340 (1999).  
[9] J. Eckert, U. Kuhn, J. Das, S. Scudino, and N. Radtke, Adv. Eng. Mater. **7**, 587 (2005).  
[10] C. Fan and A. Inoue, Appl. Phys. Lett. **77**, 46 (2000).  
[11] C. Fan, C. F. Li, A. Inoue, and V. Haas, Phys. Rev. B **61**, R3761 (2000).  
[12] T. G. Nieh, J. Wadsworth, C. T. Liu, T. Ohkubo, and Y. Hirotsu, Acta Mater. **49**, 2887 (2001).  
[13] Z. P. Lu, C. T. Liu, J. R. Thompson, and W. D. Porter, Phys. Rev. Lett. **92**, 245503 (2004).  
[14] B. Yang *et al.*, Intermetallics **12**, 1265 (2004).  
[15] J. J. Lewandowski and A. L. Greer, Nat. Mater. **5**, 15 (2006).  
[16] C. Fan, H. Choo, and P. K. Liaw, Scr. Mater. **53**, 1407 (2005).  
[17] T. Jiao, L. J. Kecskes, T. C. Hufnagel, and K. T. Ramesh, Metall. Mater. Trans. A **35**, 3439 (2004).  
[18] P. F. Peterson, M. Gutmann, T. Proffen, and S. J. L. Billinge, J. Appl. Crystallogr. **33**, 1192 (2000).  
[19] T. Egami and S. J. L. Billinge, *Underneath the Bragg Peaks: Structural Analysis of Complex Materials* (Pergamon/Elsevier, London, 2003).  
[20] C. Fan *et al.* (to be published).  
[21] *Metals Handbook* (American Society for Metals, Metals Park, OH, 1991), 10th ed., Vol. 2, pp. 581–1160.  
[22] E. Pekarskaya, C. P. Kim, and W. L. Johnson, J. Mater. Res. **16**, 2513 (2001).  
[23] D. E. Polk and D. Turnbull, Acta Metall. **20**, 493 (1972).